

Supplementary Information

Effect of Stacking Mode on Mechanofluorochromic Properties of 3-Aryl-2-Cyano Acrylamide Derivatives

Qingbao Song,^a Yongsheng Wang,^a Chenchen Hu,^b Yujian Zhang,^{b*} Jingwei Sun,^a Kunyan
Wang^b and Cheng Zhang^{a*},

College of Chemical Engineering and Materials Science,
Zhejiang University of Technology, Chaowang Road No.18, Hangzhou 310000, China
E-mail: czhang@zjut.edu.cn (C. Zhang), sciencezyj@foxmail.com (Y. J. Zhang)

General experimental section

Instrumentation:

All the solvents and reactants were used as purchased from commercialized companies without further purification.

^1H and ^{13}C NMR spectra of the desired products were recorded on a Bruker AVANCE III 500-MHz instrument (Bruker, Switzerland) using TMS as the internal standard and the CDCl_3 or the DMSO as the solvents. Mass spectroscopy was recorded with a Thermo LCQ Fleet MS spectrometer. Fluorescent measurements were recorded on a Perkin-Elmer LS-55 luminescence spectrophotometer. The Φ_f of crystal was determined by using a calibrated integrating sphere system. Powder XRD measurements were conducted on X'Pert PRO diffractometer ($\text{CuK}\alpha$) in the range $5 < 2\theta < 50$ (PANalytical, Netherlands). Differential scanning calorimetry (DSC) was performed on a TA Instruments DSC2920 at a heating rate of $10\text{ }^\circ\text{C min}^{-1}$. X-ray crystallographic intensity data were collected using Bruker SMART APEX II instrument. Digital photographs were taken by Canon 550D (Canon, Japan) digital cameras.

The synthesis method and molecular stacking features of MPCPA (*o*-, *m*- *p*-)

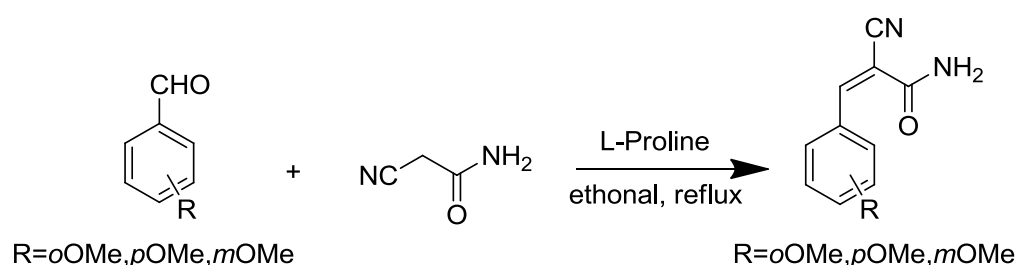


Figure S1. The synthesis method of 3-aryl-2-cyano acrylamide derivatives *o*-MPCPA, *m*-MPCP and *p*-MPCPA

2-cyano-3-(2-methoxyphenyl)-2-propenamamide (*o*-MPCPA), 2-cyano-3-(3-methoxyphenyl)-2-propenamamide (*m*-MPCPA) and 2-cyano-3-(4-methoxyphenyl)-2-propenamamide (*p*-MPCPA) were synthesized (in Chart 1) by a simple Knoevenagel reaction under gentle conditions in good yield.

A mixture of 2-(methoxy)benzaldehyde (4.08 g, 30 nmol), 2-cyanoacetamide (2.61 g, 31 nmol) and L-Proline (0.69 g, 6 nmol) in ethanol (20 ml) was heated under reflux for 2h; the solid product was filtered, washed with ethanol, dried (91% yield) and upon crystallization from ethanol solution gave rise to the pure product. Finally, the desired luminophore 2-cyano-3-(2-methoxyphenyl)-2-propenamamide (*o*-MPCPA) were fully characterized by ^1H NMR, ^{13}C NMR and HRMS. ^1H NMR (500 MHz, CDCl_3) δ 8.81 (s, 1H), 8.19 (dd, $J = 7.8, 1.2$ Hz, 1H), 7.56 -7.48 (dd, $J = 7.8, 1.6$ Hz, 1H), 7.07 (t, $J = 7.6$ Hz, 1H), 6.97 (d, $J = 8.5$ Hz, 1H), 6.35 (d, 2H), 3.91 (s, 3H). ^{13}C NMR (126 MHz, CDCl_3) δ 162.5, 159.3, 148.8, 134.7, 129.1, 120.9, 120.9, 117.4, 111.2, 102.7, 55.7. HRMS (ESI) Calcd. for $\text{C}_{11}\text{H}_{10}\text{N}_2\text{O}_2$ ($[\text{M}+\text{H}]^+$): 203.0821. Found: 203.0807. Single crystals of *o*-MPCPA was obtained by slow evaporation of ethanol/n-hexane mixtures. **Crystallographic data for *o*-MPCPA:** $\text{C}_{11}\text{H}_{10}\text{N}_2\text{O}_2$, $M = 202.21\text{ g mol}^{-1}$, monoclinic, $a = 13.7381(9)\text{ \AA}$, $b = 8.8770(4)\text{ \AA}$, $c = 17.5640(9)\text{ \AA}$, $\beta = 103.368(6)^\circ$, $V = 2083.9(2)\text{ \AA}^3$, $T = 293(2)\text{ K}$, $R_{(\text{int})} = 0.0214$, space group $I2/a$, $D_{\text{calc}} = 1.289\text{ Mg m}^{-3}$, $Z = 8$, the final R indices were $R_1 =$

0.0448, $wR_2 = 0.1153 [I > 2\sigma(I)]$, CCDC 999360.

A mixture of 3-(methoxy)benzaldehyde (4.08 g, 30 nmol), 2-cyanoacetamide (2.61 g, 31 nmol) and L-Proline (0.69 g, 6 nmol) in ethanol (20 ml) was heated under reflux for 2h; the solid product was filtered, washed with ethanol, dried (92% yield) and upon crystallization from ethanol solution gave rise to the pure product. Finally, the desired luminophore 2-cyano-3-(3-methoxyphenyl)-2-propenamide (*o*-MPCPA) were fully characterized by ^1H NMR, ^{13}C NMR and HRMS. ^1H NMR (500 MHz, CDCl_3) δ 8.31 (s, 1H), 7.54-7.48 (m, 2H), 7.42 (t, $J = 7.8$ Hz, 1H), 7.11–7.09 (m, 1H), 6.43 (s, 1H), 6.19 (s, 1H), 3.87 (s, 3H). ^{13}C NMR (126 MHz, CDCl_3) δ 162.1, 160.0, 154.1, 132.8, 130.3, 123.8, 119.7, 117.1, 114.6, 103.3, 55.4. HRMS (ESI) Calcd. for $\text{C}_{11}\text{H}_{10}\text{N}_2\text{O}_2$ ($[\text{M}+\text{H}]^+$): 203.0821. Found: 203.0822. Single crystals of *m*-MPCPA was obtained by slow evaporation of ethanol/n-hexane mixtures. **Crystallographic data for *m*-MPCPA:** $\text{C}_{11}\text{H}_{10}\text{N}_2\text{O}_2$, $M = 202.21$ g mol $^{-1}$, monoclinic, $a = 15.6778(10)$ Å, $b = 3.9598(3)$ Å, $c = 17.4076(14)$ Å, $\beta = 108.928(8)^\circ$, $V = 1022.26(13)$ Å 3 , $T = 293(2)$ K, $R_{(\text{int})} = 0.0235$, space group $P2(1)/c$, $D_{\text{calc}} = 1.314$ Mg m $^{-3}$, $Z = 4$, the final R indices were $R_1 = 0.0430$, $wR_2 = 0.1138 [I > 2\sigma(I)]$, CCDC 999359.

A mixture of 4-(methoxy)benzaldehyde (4.08 g, 30 nmol), 2-cyanoacetamide (2.61 g, 31 nmol) and L-Proline (0.69 g, 6 nmol) in ethanol (20 ml) was heated under reflux for 2h; the solid product was filtered, washed with ethanol, dried (94% yield) and upon crystallization from ethanol solution gave rise to the pure product. Finally, the desired luminophore 2-cyano-3-(4-methoxyphenyl)-2-propenamide (*o*-MPCPA) were fully characterized by ^1H NMR, ^{13}C NMR and HRMS. ^1H NMR (500 MHz, DMSO) δ 8.11 (s, 1H), 7.97 (d, $J = 8.8$ Hz, 2H), 7.79 (s, 1H), 7.72 – 7.59 (m, 1H), 7.14 (t, $J = 5.8$ Hz, 2H), 3.86 (s, 3H). ^{13}C NMR (126 MHz, DMSO) δ 163.1, 162.6, 150.1, 132.4, 124.4, 117.0, 114.8, 102.9, 55.6, 54.7. HRMS (ESI) Calcd. for $\text{C}_{11}\text{H}_{10}\text{N}_2\text{O}_2$ ($[\text{M}+\text{H}]^+$): 203.0821. Found: 203.0824. Single crystals of *p*-MPCPA was obtained by slow evaporation of ethanol/n-hexane mixtures. **Crystallographic data for *p*-MPCPA:** $\text{C}_{11}\text{H}_{10}\text{N}_2\text{O}_2$, $M = 202.21$ g mol $^{-1}$, monoclinic, $a = 3.920(2)$ Å, $b = 10.792(6)$ Å, $c = 23.124(12)$ Å, $\beta = 93.463(8)^\circ$, $V = 976.5(9)$ Å 3 , $T = 293(2)$ K, $R_{(\text{int})} = 0.1143$, space group $P2(1)/c$, $D_{\text{calc}} = 1.375$ Mg m $^{-3}$, $Z = 4$, the final R indices were $R_1 = 0.0824$, $wR_2 = 0.2367 [I > 2\sigma(I)]$, CCDC 999361.

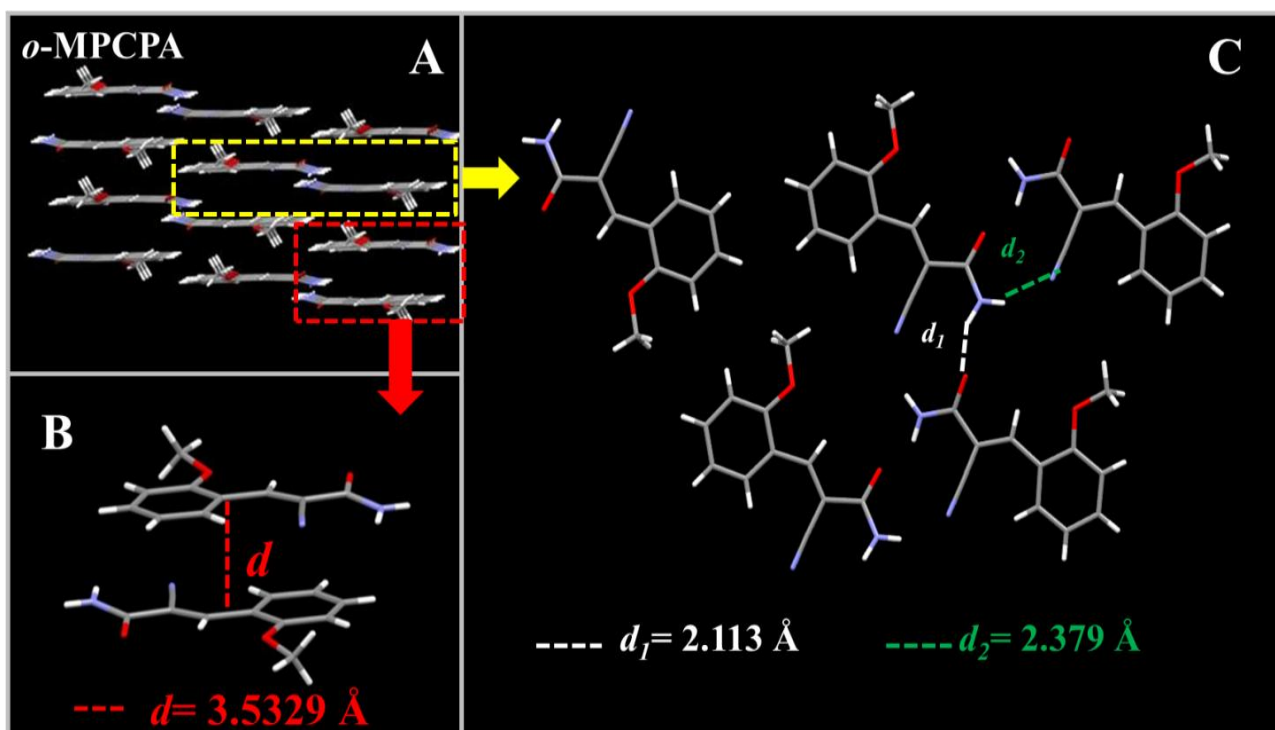


Figure S2 Crystal structures of *o*-MPCPA: (A) Side view of the antiparallel dipole arrangement. (B) View of the antiparallel arrangement along long molecular axes. (C) Top view and illustration of N-H...O (CO) and N-H...N (CN) hydrogen bonds interactions.

The crystal structure was monoclinic, space group $I2/a$, consisting of eight molecules in unit cell. As depicted in **Figure S1**, in crystal, the aromatic ring, cyano together with the acrylamide are located on the same plane. As can be seen from **Figure S1B** the luminogens *o*-MPCPA adopts the antiparallel face-to-face packing mode in order to fit into the crystalline lattice. From the top view, the aromatic ring did not overlap between the adjacent molecules (interplanar distance of 3.5329 \AA). As a result, such antiparallel H-type packing mode did not result in the π - π interactions, which contributed to enhance quantum yields of crystals. As can be seen from **Figure S1C** there were two types of N-H...O (d_1) and N-H...N (d_2) hydrogen bonds formed between two *o*-MPCPA molecules with the distance of 2.113 \AA and 2.379 \AA respectively.

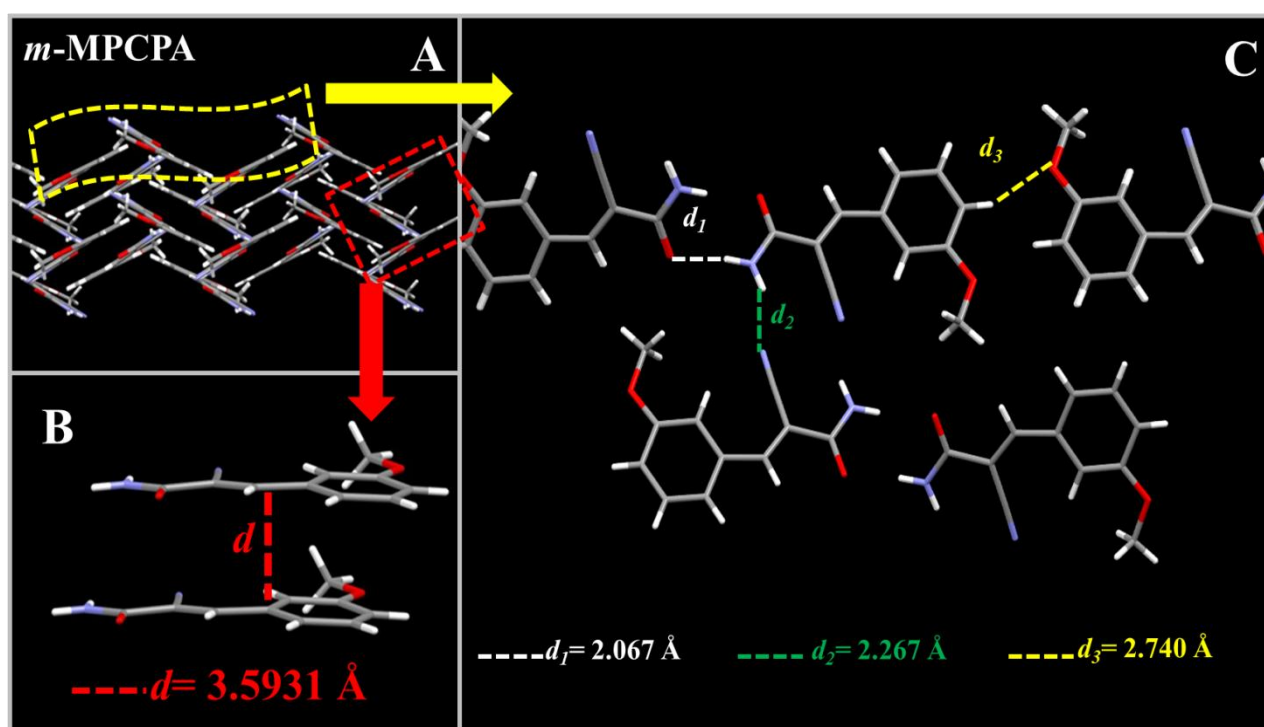


Figure S3 Crystal structures of *m*-MPCPA: (A) Side view of the antiparallel dipole arrangement. (B) View of the antiparallel arrangement along long molecular axes. (C) Top view and illustration of N-H...O (CO), N-H...N (CN) and N-H...O (CO) hydrogen bonds interactions.

and C–H...O (OCH₃) hydrogen bonds interactions.

The crystal structure was monoclinic, space group $P2(1)/c$, consisting of four molecules in unit cell. As depicted in **Figure S2**, in crystal, the aromatic ring, cyano together with the acrylamide are located on the same plane. As can be seen from **Figure S2B** the luminogens *m*-MPCPA adopts the head-to-head or parallel arrangements in order to fit into the crystalline lattice. From the top view, the inter-plane distance was less than the range of the effective intermolecular interaction (interplanar distance of **3.5931 Å**), but π – π overlap was slight reduced due to the slip-stacking along the long axis. Thus, there was a weak π – π interactions between aromatic rings, which caused fluorescence quenching. As can be seen from **Figure S2C** there were three types of N–H...O (d_1), N–H...N (d_2) and C–H...O (d_3) hydrogen bonds formed between two *m*-MPCPA molecules with the distance of **2.067 Å**, **2.267 Å** and **2.740 Å** respectively.

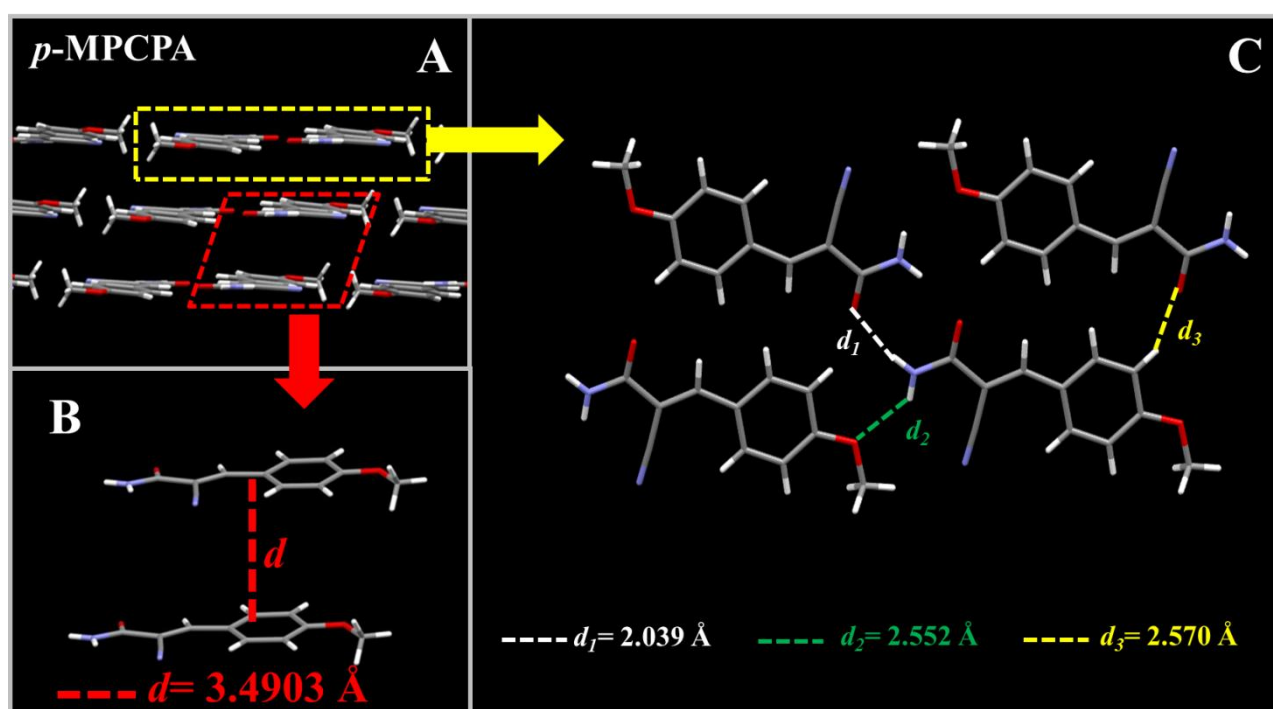


Figure S4 Crystal structures of *p*-MPCPA: (A) Side view of the antiparallel dipole arrangement. (B) View of the antiparallel arrangement along long molecular. (C) Top view and illustration of N–H...O (CO), N–H...O (OCH₃) and C–H...O (CO) hydrogen bonds interactions.

The crystal structure was monoclinic, space group $P2(1)/c$, consisting of four molecules in unit cell. As depicted in **Figure S3**, in crystal, the aromatic ring, cyano together with the acrylamide are located on the same plane. As can be seen from **Figure S3B** the luminogens *p*-MPCPA adopts the head-to-head or parallel arrangements in order to fit into the crystalline lattice. From the top view, the inter-plane distance was less than the range of the effective intermolecular interaction (interplanar distance of **3.4903 Å**), but π – π overlap was slight reduced due to the slip-stacking along the long axis. Thus, there was a weak π – π interactions between aromatic rings, which caused fluorescence quenching. As can be seen from **Figure S3C** there were three types of N–H...O (d_1), N–H...O (d_2) and C–H...O (d_3) hydrogen bonds formed between two *p*-MPCPA molecules with the distance of **2.039 Å**, **2.552 Å** and **2.570 Å** respectively.

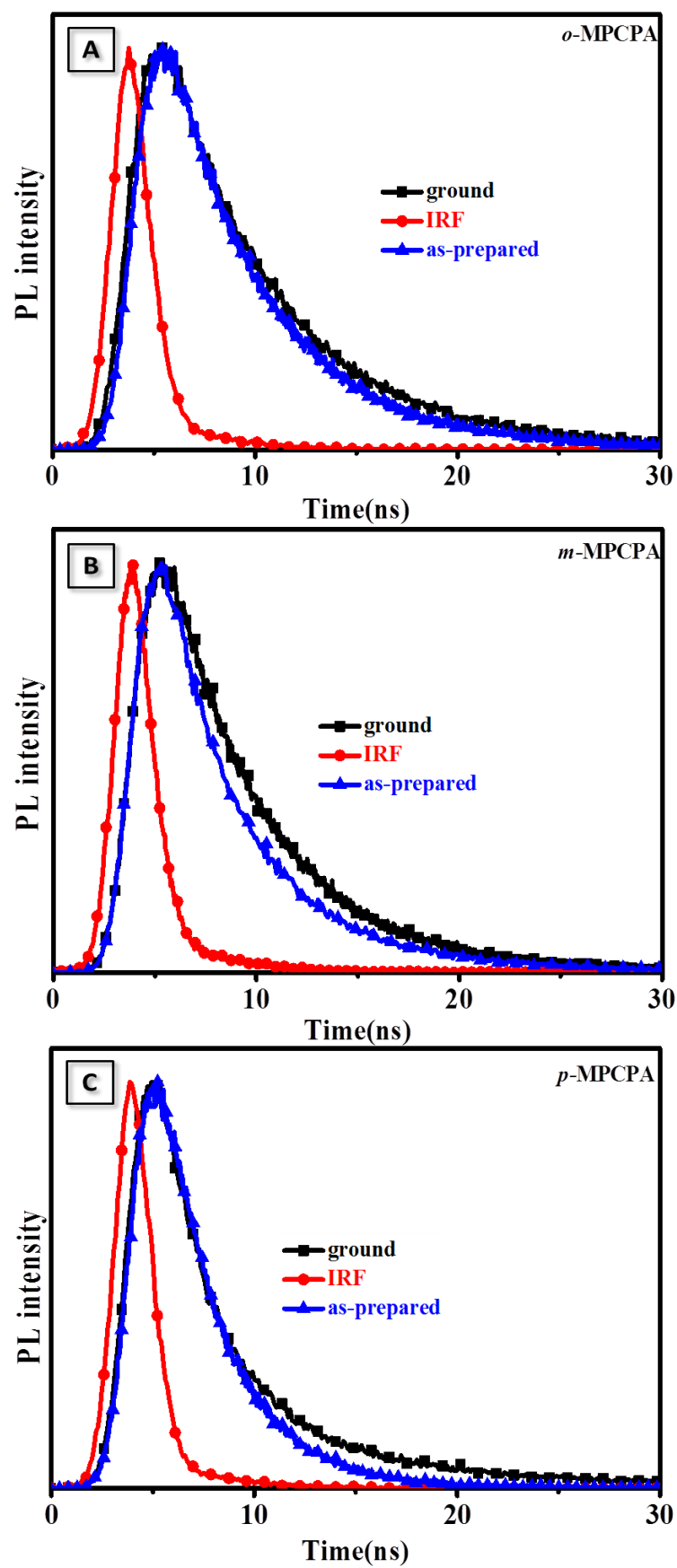


Figure S5 Fluorescence decay profiles of *o*-MPCPA (A), *m*-MPCPA (B) and *p*-MPCPA (C) at different states

Table S1. Time-resolved emission-decay curves of the crystals *o*-MPCPA, *m*-MPCPA and *p*-MPCPA samples in original and ground state with Function $I \propto \sum_i A_i \exp(-t/\tau_i)$ (A_i and τ_i are the relative weights and lifetimes respectively, $i=1, 2$). (The weighted mean lifetime $\langle\tau\rangle$ was calculated by the following equation: $\langle\tau\rangle = (A_1\tau_1 + A_2\tau_2)/(A_1 + A_2)$. The non-radiative rate constant k_{nr} was calculated by the following equation: $k_{nr} = (1-\Phi_f)/\tau_f$. The radiative rate constant k_F was calculated by the following equation: $k_F = \Phi_f/\tau_f$)

	Type	$\tau_1(\text{ns})^a$	$\tau_2(\text{ns})^a$	$A_1^b(\%)$	$A_2^b(\%)$	$\langle\tau\rangle(\text{ns})^c$	$k_{nr}(10^8\text{s}^{-1})^d$	$k_F(10^7\text{s}^{-1})^e$
<i>o</i> -MPCPA	original	4.9628	8.5760	52.05	47.95	6.23	1.2	3.7
	grinding	3.2636	8.0160	39.77	60.23	6.69	1.1	3.6
<i>m</i> -MPCPA	original	2.5237	6.1820	59.90	40.10	2.99	3.1	4.0
	grinding	3.4668	6.8089	66.00	34.00	4.61	1.9	1.7
<i>p</i> -MPCPA	original	2.1337	3.5176	65.03	34.97	2.62	3.2	6.1
	grinding	2.6584	12.6379	74.30	25.70	5.22	1.7	1.9

^a Fluorescence lifetime. ^b Fractional contribution. ^c Weighted mean lifetime. ^d Non-radiative rate constant. ^e Radiative rate constant.

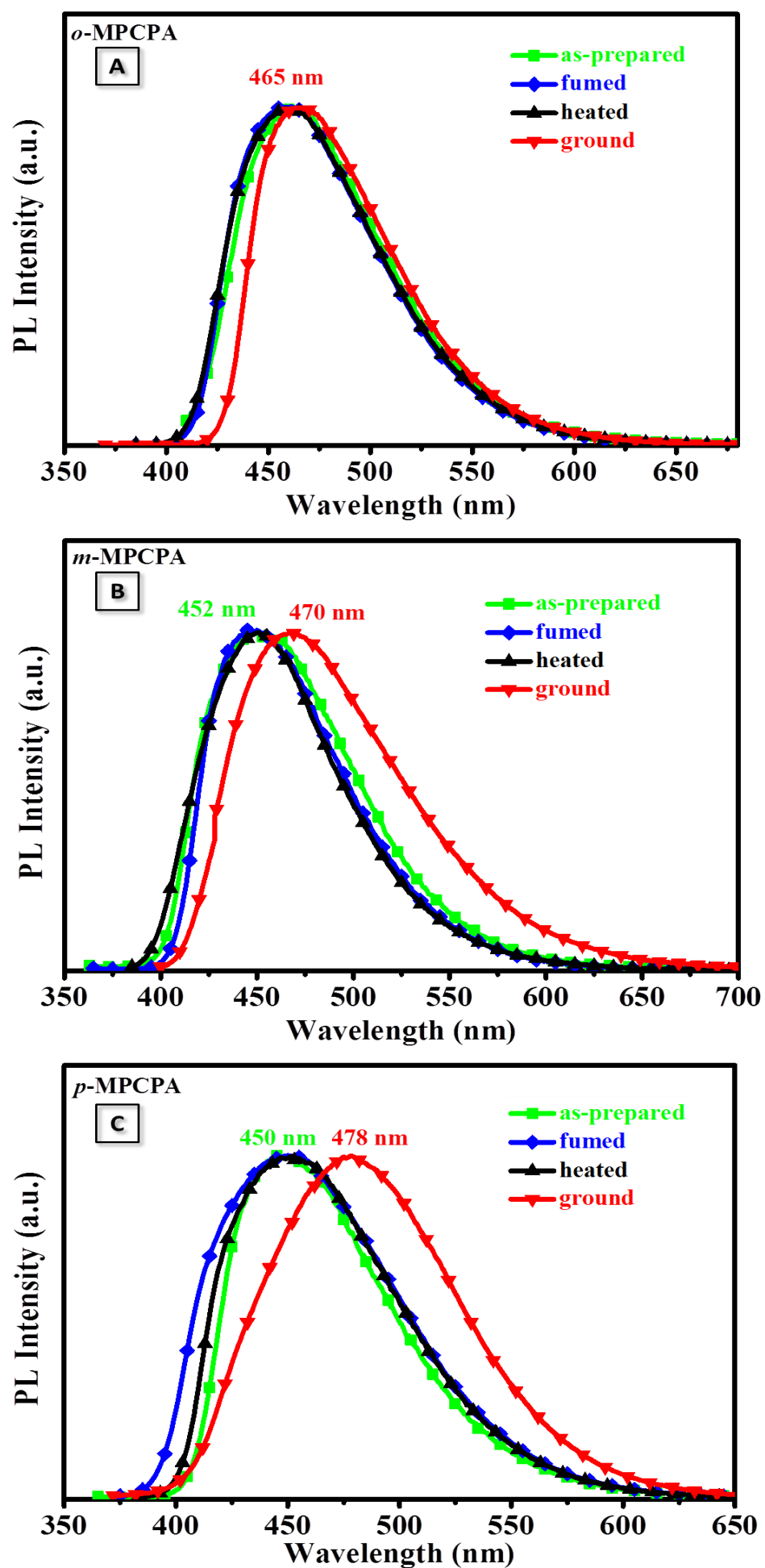


Figure S6 PL profiles of *o*-MPCPA (A), *m*-MPCP (B) and *p*-MPCPA (C) at heating treatment and fuming treatment states

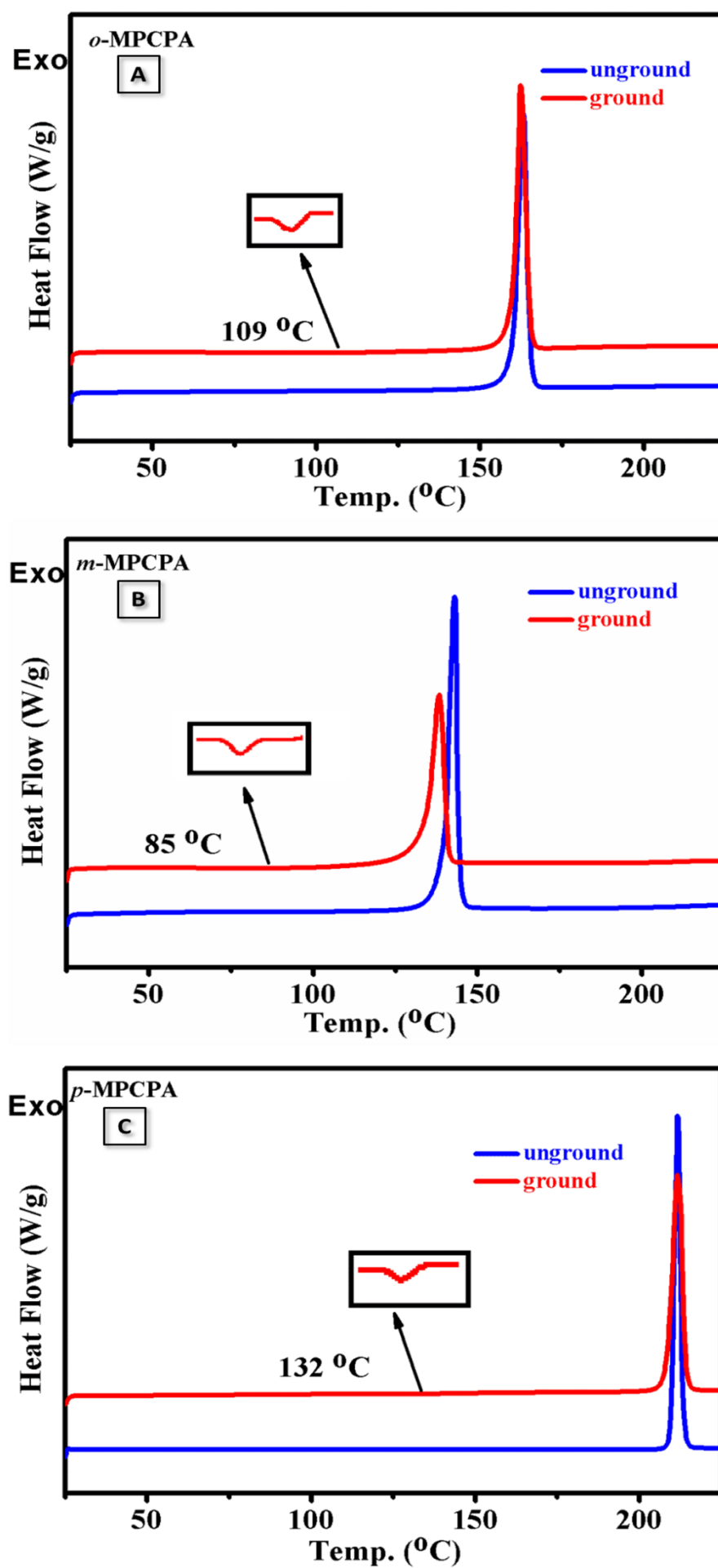
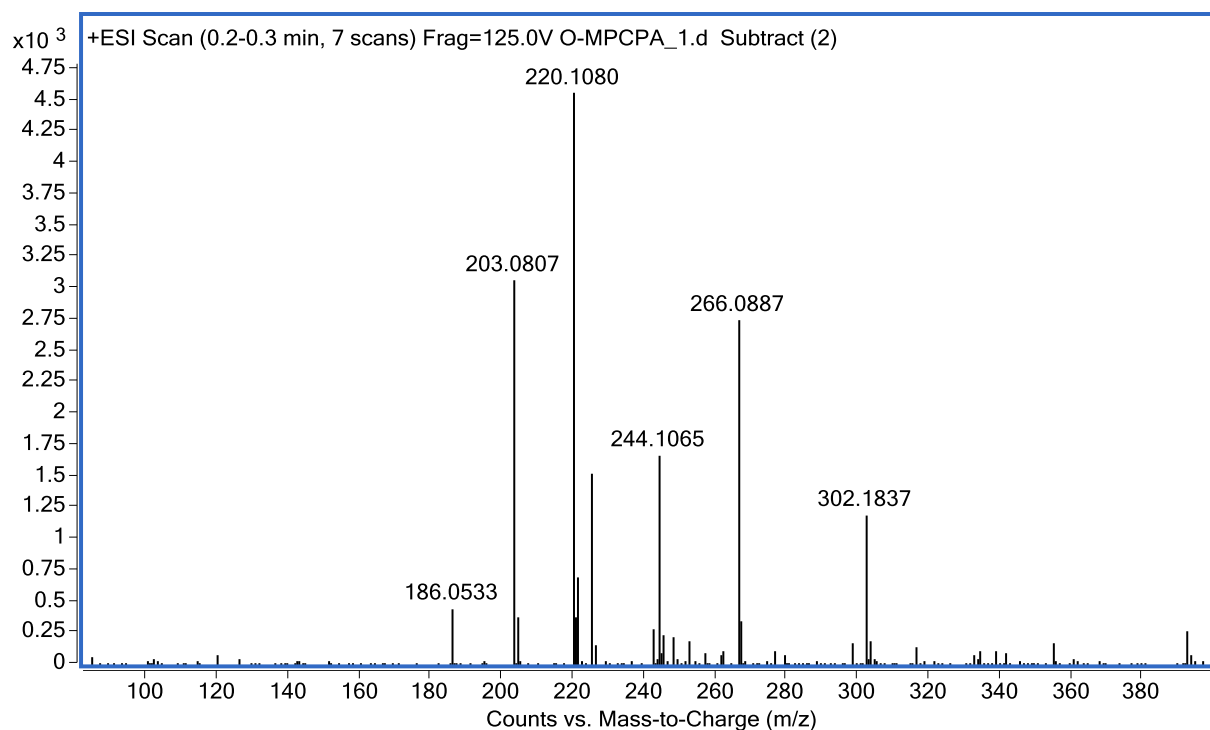


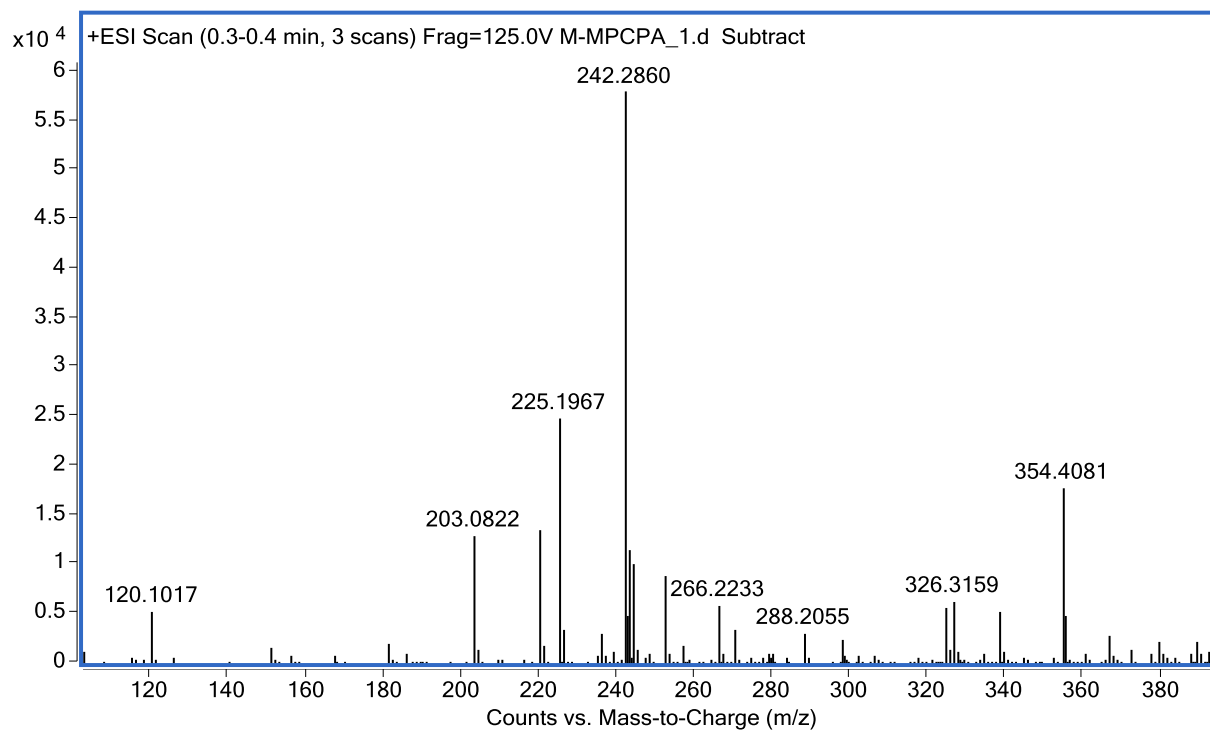
Figure S7 DSC profiles of *o*-MPCPA (A), *m*-MPCP (B) and *p*-MPCPA (C) at different states.

O-MPCPA



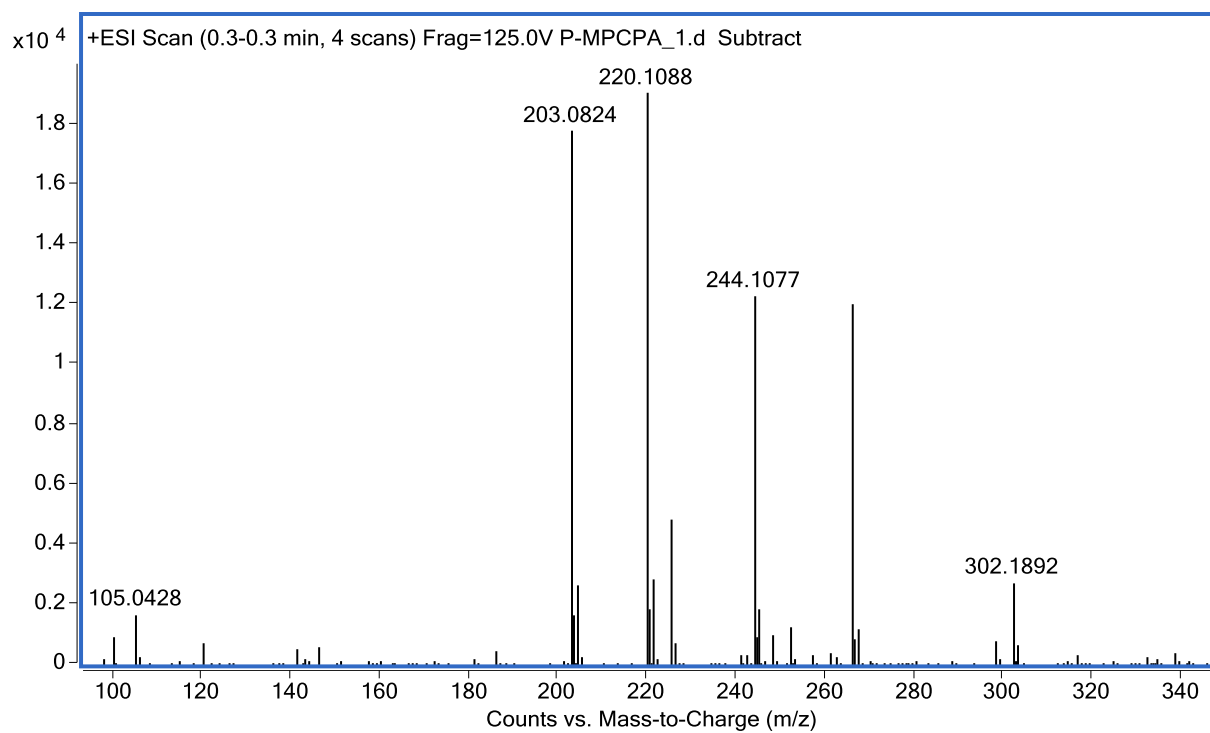
Formula (M)	Ion Formula	m/z	Calc m/z	Diff (ppm)	DBE
C11 H10 N2 O2	C11 H11 N2 O2	203.0807	203.0815	3.98	8

M-MPCPA



Formula (M)	Ion Formula	m/z	Calc m/z	Diff (ppm)	DBE
C11 H10 N2 O2	C11 H11 N2 O2	203.0822	203.0815	-3.44	8

P-MPCPA



Formula (M)	Ion Formula	m/z	Calc m/z	Diff (ppm)	DBE
C11 H10 N2 O2	C11 H11 N2 O2	203.0824	203.0815	-4.43	8